IOPscience iopscience.iop.org

Home Search Collections Journals About Contact us My IOPscience

Multifrequency EPR study of Cr^{3+} ions in $LiScGeO_4$

This article has been downloaded from IOPscience. Please scroll down to see the full text article.

2000 J. Phys.: Condens. Matter 12 4465

(http://iopscience.iop.org/0953-8984/12/20/302)

View the table of contents for this issue, or go to the journal homepage for more

Download details:
IP Address: 171.66.16.221
The article was downloaded on 16/05/2010 at 04:54

Please note that terms and conditions apply.

J. Phys.: Condens. Matter **12** (2000) 4465–4473. Printed in the UK PII: S0953-8984(00)12052-1

Multifrequency EPR study of Cr^{3+} ions in $LiScGeO_4$

A A Galeev†‡, N M Khasanova†‡, C Rudowicz†¶, G S Shakurov§, A B Bykov‖, G R Bulka‡, N M Nizamutdinov‡ and V M Vinokurov‡

† Department of Physics and Materials Science, City University of HK, Kowloon Tong, Hong Kong SAR
‡ PhMA Laboratory, Kazan State University, 18 Kremlevskaya Street, Kazan 420008, Russia
§ Kazan Physical-Technical Institute, RAS, Sibirsky trakt 10/7, Kazan 420029, Russia
‖ Shubnikov Institute of Crystallography, RAS, Moscow 117333, Russia

E-mail: apceslaw@cityu.edu.hk (C Rudowicz)

Received 23 February 2000

Abstract. An electron paramagnetic resonance study of a synthetic single crystal of Cr-doped $LiScGeO_4$ was carried out at the X- and Q-bands at 300 K and at the broad band (70–370 GHz) at 4.2 K. It was established that the EPR spectra with the magnetic multiplicity $K_M = 2$ observed in all the frequency bands are due to the Cr^{3+} substituted for Sc^{3+} at the mirror symmetry octahedral site. The angular dependences of the two symmetry-related spectra of Cr^{3+} in the three crystallographic planes were fitted with the spin Hamiltonian ($S = 3/2$) of monoclinic symmetry. The zero-field splitting of the ground state energy levels was determined as 1.309(5) cm^{-1} which compares well with that for Cr^{3+} in forsterite and alexandrite crystals with similar olivine-like structure. Additional weak lines due to Mn^{2+} and Fe^{3+} at the mirror symmetry sites were also identified in the X- and Q-band spectra.

1. Introduction

The lithium scandium germanate $LiScGeO_4$ [1] is a new representative of materials with the olivine structure [2] and exhibits potential for laser media applications. The structure of $LiScGeO_4$ belongs to the orthorhombic space group D_{2h}^{16}—$Pnma$ (space group No 62 [3]) with $a = 1.0673$ nm, $b = 0.599\,26$ nm, $c = 0.496\,67$ nm [4]. There are three structurally non-equivalent cationic sites in $LiScGeO_4$, namely: Li^+ (4a site) and Sc^{3+} (4c site) in the octahedral, and Ge^{4+} (4c site) in the tetrahedral environment of oxygen ions [4]. Cr-doped $LiScGeO_4$ reveals optical characteristics similar to those of forsterite Mg_2SiO_4 [1]. Cr-activated forsterite (Mg_2SiO_4) [5] and alexandrite (Al_2BeO_4) [6], both with similar olivine structure, are well known tunable solid state lasers. Electron paramagnetic resonance (EPR) and optical studies of forsterite have established that Cr^{2+} [7, 8] and Cr^{3+} [9] impurity ions substitute at both the 4a and 4c octahedral sites, whereas Cr^{4+} [10] substitutes at the 4c tetrahedral site. Cr^{3+} ions in alexandrite were identified [11–13] at both the 4a and 4c octahedral sites. The optical characteristics and laser action of these crystals are sensitive to the site distribution of chromium ions and the presence of other impurities [5, 14–16].

¶ Corresponding author.

0953-8984/00/204465+09$30.00 © 2000 IOP Publishing Ltd

In this work an EPR study of Cr-doped $LiScGeO_4$ crystal [1] was carried out at the X-, Q-bands at 300 K and the high-frequency bands at 4.2 K. The aim was to obtain information on the mechanism of substitution of Cr ions. The spin Hamiltonian (SH) parameters describing the Cr^{3+} EPR spectra are determined and the site of Cr^{3+} ions is identified.

2. Multifrequency EPR spectra of single crystal of $LiScGeO_4$

Green-coloured single crystals of $LiScGeO_4$ doped with Cr^{3+} were grown by the flux method [1]. Samples for the EPR studies were preliminary oriented using the x-ray technique. Below we summarize the EPR experimental results in the three frequency bands studied.

The *X-band* ($\nu = 9.272$ GHz) spectra recorded along the a, b and c crystal axes at room temperature are presented in figure 1. Each spectral line (figure 1) is single when the external magnetic field is oriented in the ab and bc plane, but is split into two lines for other orientations thus indicating that the magnetic multiplicity [17] $K_M = 2$ for all observed spectra. In accordance with the space group D_{2h}^{16}—$Pnma$ of the crystal, $K_M = 2$ indicates that all paramagnetic ions occupy the sites 4c with the point symmetry m (the plane ac being the mirror plane). The intensity and linewidth of the observed transitions vary significantly with the crystal orientation in an external magnetic field ($\boldsymbol{B}_0$). At some orientations the existence of typical weak hyperfine satellites from the ^{53}Cr isotope ($I = 3/2$) was observed for the most intense lines (figure 1). Because of the broadness of the spectral lines, only the outer two from four hyperfine components were resolved with the separation between 5 and 5.5 mT, which is typical for ^{53}Cr. Note that at the X-band additionally more than five hyperfine sextets split by $\sim$8.7 mT (figure 1) were observed, which can be reliably attributed to $^{55}Mn^{2+}$ centres located at the 4c sites. Because of the low intensity it was not possible to study these Mn spectra in detail. The lines with no hyperfine components in figure 1 were preliminarily assigned to Fe^{3+} at the 4c octahedral and tetrahedral sites.

The *Q-band* ($\nu = 36.656$ GHz) EPR angular dependence of the Cr lines in the three crystallographic planes was studied at room temperature (figure 2). In contrast to the X-band spectra there are more transitions observed at the Q-band and a representative number of experimental lines were collected for fitting the spin-Hamiltonian parameters. As at the X-band, significant anisotropy in the transition intensity was observed for some transitions. For example, the transition 2–3 (figure 2) vanishes virtually between 5 and 7 degrees from the c-axis in the ac-plane. This feature provides an opportunity for an additional check of the fitted spin-Hamiltonian parameters by analysing how well they can describe the observed decrease in the transition intensity (see section 3). Similarly to the X-band spectra also at the Q-band additional hyperfine sextets due to $^{55}Mn^{2+}$ as well as some lines with no hyperfine components due to Fe^{3+} ions were observed and characterized by $K_M = 2$. A detailed analysis of the angular dependence of the additional Fe^{3+} spectra at the Q-band will be carried out in a separate paper.

The *broad-band* EPR [18] investigations in the frequency range 70–370 GHz at 4.2 K and magnetic field up to 1 T were carried out to verify the possible presence of the integer-spin ions Cr^{2+} ($S = 2$) and Cr^{4+} ($S = 1$) usually exhibiting a large zero-field splitting (ZFS). The angular dependence of two Cr^{3+} transitions was well observed (figure 3) when the polarization of the oscillating field ($\boldsymbol{B}_1$) was normal to $\boldsymbol{B}_0$. For this polarization an additional single isotropic line was observed in this frequency range corresponding to the ZFS of about 2.6 cm^{-1}, which can be tentatively attributed to a non-Kramers ion. However because of the broadness ($\sim$70 mT) and weakness of this line, an unambiguous determination of its nature requires additional experiments. New crystals synthesized at proper conditions would also be required. No transitions were detected in the whole frequency range using the parallel mode ($\boldsymbol{B}_1 \| \boldsymbol{B}_0$).

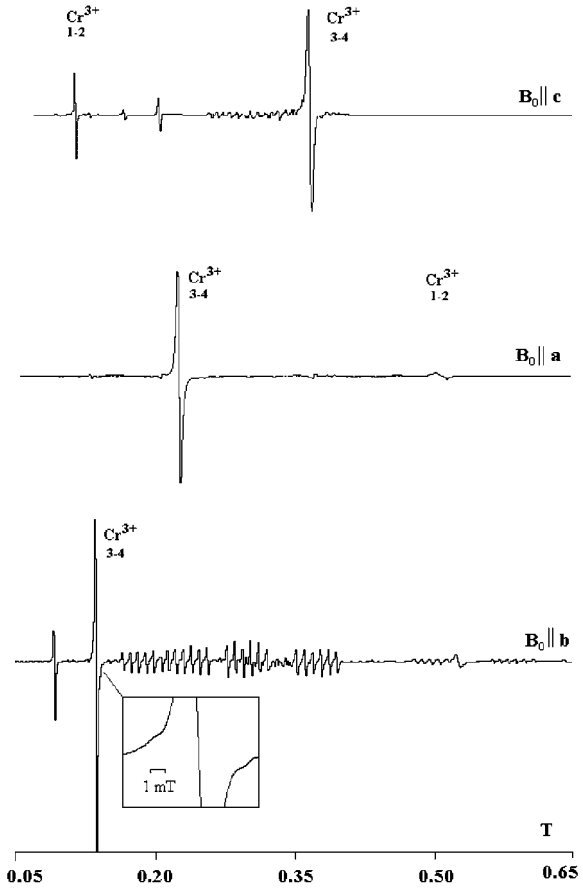

Figure 1. X-band EPR spectra of an $LiScGeO_4$ crystal along the crystallographic ($Pnma$) a, b and c axes at room temperature recorded using a PS100.X automated spectrometer. Transition lines of the Cr^{3+} centre are denoted by two numbers as indicated on the energy level diagram in figure 4.

3. SH analysis for Cr^{3+} in $LiScGeO_4$

In accordance with experimentally determined $K_M = 2$ corresponding to the site symmetry m of the space group D_{2h}^{16}—$Pnma$ [3] we use the SH expressed in the axis system $x \| c$, $y \| a$ and $z \| b$ with the z-axis normal to the ac symmetry plane which defines the monoclinic direction in the crystal [19, 20]. The spin Hamiltonian ($S = 3/2$) of the Laue symmetry C_{2h} in the (xyz) axis system is given by [21–23]:

$$H = \mu_B \left(\sum B_i g_{ii} \hat{S}_i + B_x g_{xy} \hat{S}_y \right) + B_{20} \bar{T}_{20} + B_{22} \bar{T}_{22} + B_{2-2} \bar{T}_{2-2} \tag{1}$$

where the summation index i denotes x, y, z for the diagonal Zeeman terms and B_{20}, $B_{2\pm2}$ are the *real* ZFS parameters at the corresponding linear combinations of the irreducible tensor operators [22–25] T_{LM} defined by Koster and Statz [24] and Buckmaster *et al* [25] (i.e. the KS/BCS notation [21]):

$$\bar{T}_{20} = T_{20}(\boldsymbol{S})$$
$$\bar{T}_{22} = T_{22}(\boldsymbol{S}) + T_{2-2}(\boldsymbol{S}) \qquad \bar{T}_{2-2} = \mathrm{i}[T_{22}(\boldsymbol{S}) - T_{2-2}(\boldsymbol{S})]. \tag{2}$$

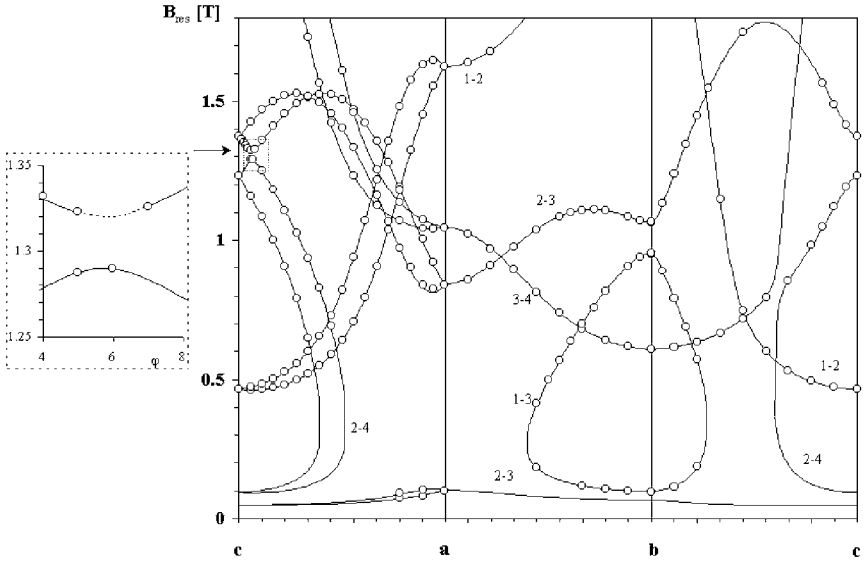

Figure 2. Angular dependence of the Cr^{3+} Q-band EPR transitions at room temperature in the three crystallographic planes. Circles denote the experimental data, whereas the curves are calculated using the SH parameters listed in table 1. Two numbers denote the transitions according to the energy level notation indicated in figure 4. The inset illustrates the vanishing of the transition 2–3 (broken curve) in the vicinity of the principal axis of the ZFS tensor (table 2).

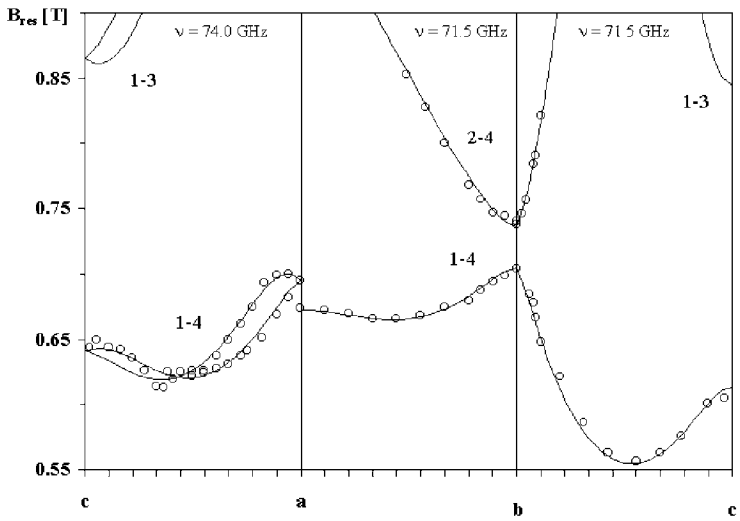

Figure 3. Angular dependence of the Cr^{3+} high-frequency EPR transitions at 4.2 K in the three crystallographic planes. Circles denote the experimental data, whereas the curves are calculated using the SH parameters listed in table 1. Two numbers denote the transitions according to the energy level notation indicated in figure 4.

The linear combinations of the spin operators in the equation (2) belong to the category of the 'normalized combinations of spherical tensor (NCST) operators' [21]. The parameters B_{2M} [22, 23] in equation (1) turn out to be equivalent to those in the KS/BCS [24, 25] notation

Table 1. SH parameters for Cr^{3+} in $LiScGeO_4$. B_{LM} and b_k^q are in the units of 10^{-4} cm^{-1}; S_2 in cm^{-2}; Δ in cm^{-1}; angles are in degrees. The rms deviation $\varepsilon = \sqrt{\sum_{i=1}^{N} \Delta B_i^2 (N-p)}$ of the measured and the computed resonance magnetic fields was obtained for a fit of $p = 7$ parameters over $N = 124$ transitions involved.

Values in the axis system $x\|c$, $y\|a$, $z\|b$ (the space group $Pnma$)			Principal values of the ZFS tensor and the orientation of principal axis system (XYZ) referred to the (xyz) axis system	
ZFS parameters				
M, q	B_{2M}	b_2^q	$\alpha = 5.68^\circ$, $\beta = 90^\circ$, $\gamma = 90^\circ$	
0	3835.92	4698.02	$B_{20} = -5142.95$	$b_2^0 = -6298.802$
2	−2581.62	−7744.86	$B_{22} = -1032.415$	$b_2^2 = -3097.245$
−2	518.60	−1555.80	$B_{22}/B_{20} = 0.20$	$b_2^2/b_2^0 = 0.49$
g-tensor components				
$g_{xx} = 1.97(412)$ $g_{xy} = -0.00(203)$				
$g_{yy} = 1.97(217)$ $g_{zz} = 1.97(679)$				
$N = 124$; $\varepsilon = 1.3$ (mT), $\Delta = 1.309(54)$ cm^{-1}; $S_2 = 0.285$ cm^{-2}				

[21] for the SH expressed in the *expanded* form [21]. The B_{LM} parameter are related to the extended Stevens (ES) ones b_k^q [21], which are the most commonly used in EPR practice, as follows:

$$B_{20} = (2/\sqrt{6})b_2^0 \qquad B_{22} = (1/3)b_2^2. \tag{3}$$

The rotational invariant of the ZFS tensor defined in the equation (1) is given by:

$$S_2 = (B_{20})^2 + 2\sum_{M\neq 0}(B_{2M})^2. \tag{4}$$

All SH parameters listed in table 1 were obtained by fitting the Q-band spectral angular dependence in the three crystallographic planes ab, bc and ac using the modified program [26]. In the coordinate system rotated around the z-axis through the angle $\phi = -\tan^{-1}(B_{2-2}/B_{22})/2 = 5.68^\circ$ the parameter B_{2-2} is reduced to zero yielding the ZFS tensor represented by the principal values only: $B_{20} = 3835.92$ and $B_{22} = -2633.19$ (in 10^{-4} cm^{-1}) with the ratio $\lambda' \equiv b_2^2/b_2^0 = \sqrt{6}B_{22}/B_{20} = -1.68$. Note that the angle $\phi = 5.68^\circ$ is a measure of monoclinicity [19, 20] since it describes the strength of the monoclinic distortion. The value of λ' is, however, out of the standard range ($0 \leqslant \lambda' \leqslant 1$) and requires the transformation S4 [27, 28] to satisfy the orthorhombic standardization [27]. The program [26] yields the same standardized results due to the built-in diagonalization procedure for the second-rank ZFS tensor. Hence, in table 1 the orientation of the principal axis system for the ZFS tensor is given by the Euler angles describing transformation of the initial (xyz) axis system to the new (XYZ) one satisfying the standardization requirement ($\lambda' = 0.49$).

To facilitate comparison with other experimental data, the ZFS parameters in table 1 are also given in the ES notation [21]. The sign of B_{20} was not determined experimentally, since all measurements were carried out at fixed room and liquid helium temperatures. The energy level diagrams are presented in figure 4 together with the energy difference plots.

When $\boldsymbol{B}_0$ is along the c-axis ($Pnma$), the two Q-band transitions 2–3 and 2–4 appear in the vicinity of the energy level crossing at 1.35 T, as seen from figure 4. Using the SH parameters in table 1 we calculated the mixing coefficients in the linear combination of the spin functions by a numerical diagonalization of the SH matrix. The transition probabilities P_{ij} and the relative intensities I_{ij} [29] for the transitions 2–3 and 2–4 with $\boldsymbol{B}_0$ in the ac-plane in the vicinity of the principal axis direction of the ZFS tensor (table 1) and $\boldsymbol{B}_1$ along the b-axis were

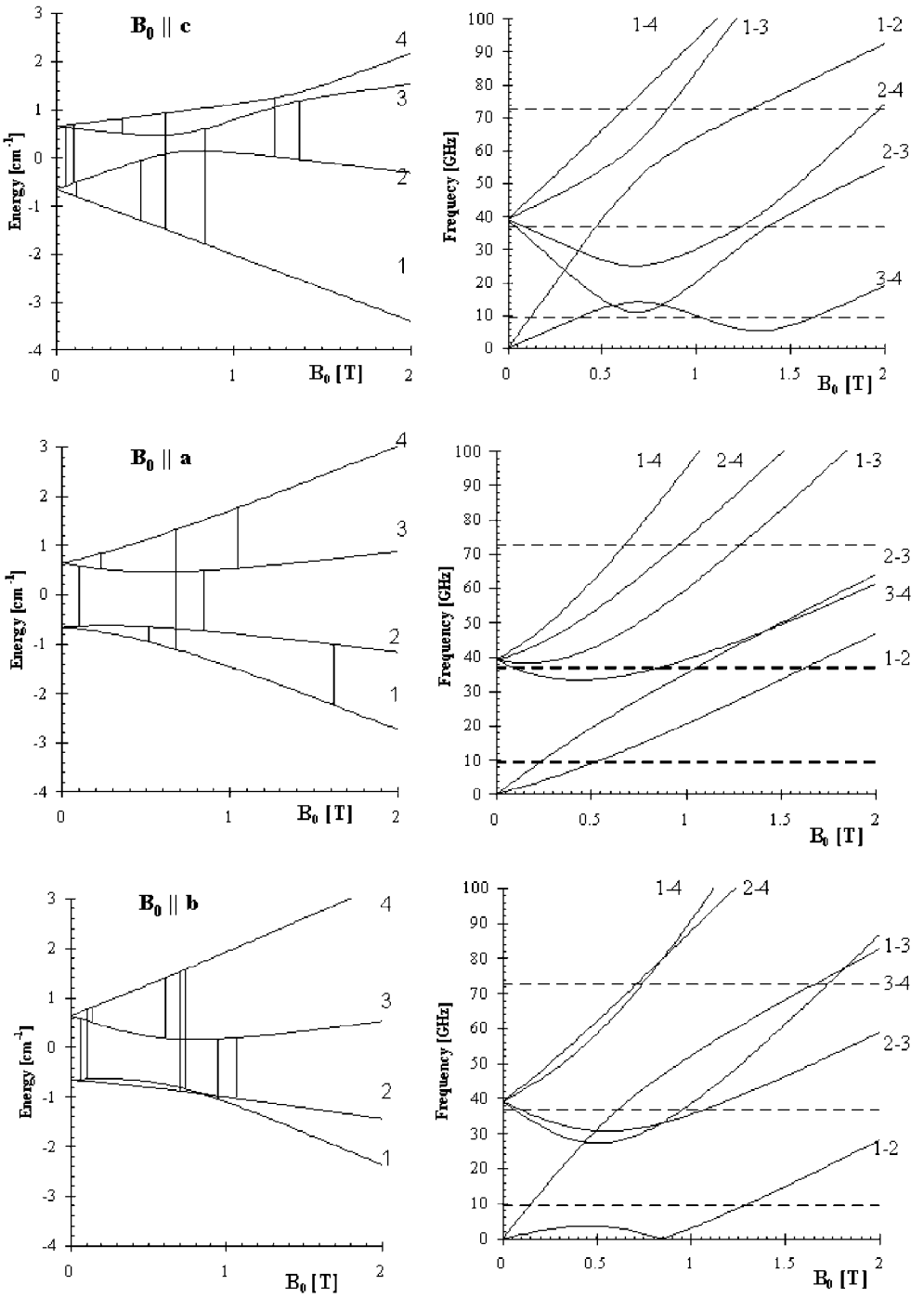

Figure 4. Energy level and resonance frequency diagrams for Cr^{3+} in $LiScGeO_4$ with the magnetic field B_0 along the crystallographic axes. For convenience, the numbers from 1 to 4 in the order of increasing energy denote the states, whereas two respective numbers denote the transitions between the two levels involved. Vertical lines between the energy levels indicate the observed transitions. Broken horizontal lines on the frequency diagrams indicate the three resonance frequencies used in this study (see figures 1–3).

Table 2. Calculated values of the resonance magnetic field $\boldsymbol{B}_{res}$ (in 10^{-4} T), probability P_{ij} and intensity I_{ij} of the vanishing (2–3) and non-vanishing (3–4) Cr^{3+} transitions in the ac-plane in the vicinity of the principal Z-axis direction of the ZFS tensor transitions shown in the inset of figure 2. The angle φ is measured from the c-axis in the ac-plane.

	Transition 2–3			Transition 2–4		
$\varphi^{(\circ)}$	$\boldsymbol{B}_{res}$	P_{23}	I_{23}	$\boldsymbol{B}_{res}$	P_{24}	I_{24}
0	13 746.7	0.7612	2.0037	12 297.1	0.8972	2.1231
5	13 233.7	0.1315	0.4604	12 887.1	1.5448	3.0016
5.7	13 208.6	**0.0003**	**0.0012**	12 913.7	1.6763	3.1325
6	13 212.5	0.0217	0.0808	12 910.1	1.6549	3.1119
7	13 275.9	0.2819	0.9122	12 844	1.3939	2.8364
10	13 592.4	0.6834	1.8511	12 492.8	0.9835	2.274

calculated as listed in table 2. The values P_{23} and I_{23} explain well experimentally observed vanishing of the transition line 2–3 between 5 and 7° from the c-axis in the ac-plane, thus providing an additional confirmation of the reliability of the fitted SH parameters in table 1.

4. Discussion and conclusions

The EPR study at various frequency bands of the Cr-doped $LiScGeO_4$ allowed us to obtain a representative set of experimental spectra indicating (i) major lines, which were identified as due to Cr^{3+}, and (ii) additional lines due to Mn^{2+} and Fe^{3+} ions. The presence of these additional impurities in low concentration is not surprising because they are usual traces in the natural and synthetic crystals with olivine-like structure. The fact that the EPR spectra of Mn^{2+} both at the X- and Q-band reveal more than five fine structure components observed along the crystallographic axes suggests that several Mn centres in $LiScGeO_4$ exist, each differing in the charge compensation mechanisms at the Mn^{2+} substitution sites. Preliminary analysis of the Fe^{3+} lines in the X- and Q-band EPR spectra shows that Fe^{3+} impurity substitutes at the two structurally non-equivalent 4c sites in $LiScGeO_4$.

The Cr^{3+} EPR spectra exhibit monoclinic symmetry and were fitted using a monoclinic spin Hamiltonian. Determination of the SH parameters for Cr^{3+} ions has enabled identification of their substitution sites. The diagonal components of the $\boldsymbol{g}$ tensor in table 1 are typical for Cr^{3+} in a similar octahedral environment [12, 30], whereas overall the $\boldsymbol{g}$ tensor is nearly isotropic for Cr^{3+} in $LiScGeO_4$. The main contribution to the spectrum anisotropy comes from the relatively large ZFS parameters. Cr^{3+} ions are found to exhibit the zero-field splitting $\Delta \sim 39.2$ GHz (1.309 cm^{-1}), which is larger than the usual Q-band frequency. The fitted SH parameters for $S = 3/2$ (table 1) account well for the experimental angular dependence of the EPR spectra observed in all the three frequency bands studied. The observed weak hyperfine components with separation typical for ^{53}Cr (9.54% natural abundance) allow us to identify unambiguously that the spectral lines are due to the Cr^{3+} ($S = 3/2$) paramagnetic centres. From the symmetry of the spectrum indicating the magnetic multiplicity $K_M = 2$ and the well known strong preference of Cr^{3+} for hexacoordinate and octahedral complexes (see, e.g., [31]) we conclude that the Cr^{3+} ions substitute for Sc^{3+} and thus do not require a charge compensation. A general difficulty in firm assignment of each of the two symmetry related Cr^{3+} EPR spectra to one of the two symmetry-related octahedral 4c sites arises from the low value of spin $S = 3/2$ and thus the existence of only the second rank ZFS tensor. For Fe^{3+} with $S = 5/2$ useful structural information can be obtained from the topological (pseudosymmetry) analysis of the fourth

rank ZFS tensor [22, 23, 26]. Additional confirmation of our present conclusion on the Cr^{3+} substituting for Sc^{3+} would be possible by performing the full diagonalization of the crystal field Hamiltonian [32, 33] within the $3d^3$ configuration as in the case of Cr^{3+} in aluminosilicates [34, 35]. This procedure involves the optical parameters, which are not available at present for the Cr-doped $LiScGeO_4$.

The fact that EPR spectra obtained at 4.2 K and room temperature can be well described by the same set of the SH parameters indicates that within the experimental accuracy no temperature dependence is observed. Hence no structural changes occur in this temperature range in the $LiScGeO_4$ crystal. This stability of the structure is an important factor for laser media applications.

In order to extract more structural information from our data it is worthwhile to compare the zero field splitting (Δ) determined for Cr^{3+} in $LiScGeO_4$ with that for Cr^{3+} in other structurally similar crystals. The value $\Delta = 1.309\ cm^{-1}$ in table 1 is of the same order of magnitude as for Cr^{3+} at the 4c octahedral sites in forsterite: $1.44\ cm^{-1}$ [9] and alexandrite: $0.53\ cm^{-1}$ [11–13]. The principal Z-axis of the ZFS tensor for Cr^{3+} in $LiScGeO_4$ (table 1) deviates by only ± 5.68 degrees from the crystallographic c-axis along which the occupied and unoccupied octahedral 4c sites are alternately located in this crystal structure. This deviation is comparable to that for Cr^{3+} substituted for Mg^{2+} in forsterite: ± 3 degrees [9] and for Cr^{3+} substituted for Al^{3+} in alexandrite: ± 3.65 degrees [11–13] at the same octahedral 4c sites. Note that in the case of the Cr^{3+}–Al^{3+} pair centre [30] with mirror symmetry in forsterite this deviation from the c-axis: ± 7.3 degrees [29] is only slightly larger due to the presence of the charge compensating substitution of Al^{3+} for Si^{4+} in one of the nearest tetrahedral sites. The closeness of (i) the values of the Cr^{3+} ZFS parameters and (ii) the directions of the principal axes emphasizes the common feature of the Cr^{3+} substitution at the mirror symmetry octahedral sites in the three similar crystals with the olivine-like structure.

It is worthwhile to note that the EPR studies of forsterite [9, 30] reveal that Cr^{3+} ions substitute for Mg at both the 4a and 4c octahedral sites with a preference for the 4a sites. In alexandrite the chromium ions substitute for Al at each of the two octahedral sites with a preference for the 4c octahedral sites [16]. In contrast to these crystals, in the case of $LiScGeO_4$ we have not detected any low symmetry EPR spectra with the magnetic multiplicity $K_M = 4$, which would originate from Cr ions or other transition ions substituted at the 4a sites. This reduces the number of possible optically active centres, which have to be taken into account for full understanding of the optical absorption and luminescence properties of the Cr-doped $LiScGeO_4$ crystal [1].

Acknowledgments

We wish to express our sincere gratitude to V A Shustov for the x-ray measurements. This work was supported by the RGC and the City University of Hong Kong through the research grant SRG 7000768.

References

[1] Bykov A B, Kanunnikov G V and Bratys A L 1993 *Inorg. Mater.* **29** 278
[2] Birle J D, Gibbs G V, Moore P B and Smith J V 1968 *Am. Mineral.* **53** 807
[3] Hahn Th (ed) 1987 *International Tables for Crystallography* 2nd rev. edn. (Dordrecht: Kluwer) p 288
[4] Genkina E A, Timofeeva V A and Bykov A B 1986 *Zh. Strukt. Khim.* **27** 167
[5] Petricevic V, Gayen S K and Alfano R R 1988 *Appl. Phys. Lett.* **53** 2590
[6] Walling J C, Peterson O G, Jenssen H P, Morris R C and O'Dell E W 1980 *IEEE J. Quantum Electron.* **16** 1302
[7] Tarasov V F, Shakurov G S and Gavrilenko A N 1997 *Phys. Solid State* **37** 270

[8] Casas-Gonzalez J, Jacobsen S M, Hoffman K R and Yen W M 1991 *OSA Proc. Advanced Solid-State Lasers* vol 10, ed G Dube and L Chase (Washington, DC: Optical Society of America) p 64
[9] Rager H 1977 *Phys. Chem. Miner.* **1** 371
[10] Hoffman K R, Casas-Gonzalez J, Jacobsen S M and Yen W M 1991 *Phys. Rev.* B **44** 12 589
[11] Barry W R and Troup G J 1969 *Phys. Status Solidi* **35** 861
[12] Forbes C E 1983 *J. Chem. Phys.* **79** 2590
[13] Khasanova N M, Nizamutdinov N M, Bulka G R, Khasanov R A, Garmash V M, Ermakov G A and Vinokurov V M 1985 *Physics of Rock Minerals* ed V Vinokurov (Kazan State University Press) p 11
[14] Sugimoto A, Nobe Y, Yamazaki T, Yamaguchi Y, Yamagushi K, Segawa Y and Takei H 1997 *Phys. Chem. Miner.* **24** 333
[15] Hasan Z and Manson N B 1988 *J. Phys. C: Solid State Phys.* **21** 3351
[16] Rager H, Bakhshandeh-Khiri A and Schmetzer K 1998 *N. Jb. Miner. Mh.* **12** 545
[17] Nizamutdinov N M, Bulka G R, Gainullina N M and Vinokurov V M 1976 *The Physical Properties of Minerals and Rocks* ed V Vinokurov (Kazan State University Press) p 3
[18] Tarasov V F and Shakurov G S 1991 *Appl. Magn. Reson.* **2** 571
[19] Misra S K and Rudowicz C 1988 *Phys. Status Solidi* b **147** 677
[20] Rudowicz C 1998 *Proc. Int. Conf. on Spectroscopy, X-Ray and Crystal Chemistry of Minerals (Kazan, 1997)* ed A Bakhtin (Kazan University Press) p 31
[21] Rudowicz C 1987 *Magn. Reson. Rev.* **13** 1; Erratum 1988 *Magn. Reson. Rev.* **13** 335
[22] Khasanova N M, Nizamutdinov N M, Vinokurov V M and Bulka G R 1988 *Sov. Phys.–Crystallogr.* **33** 527
[23] Vinokurov V M, Gaite J M, Bulka G R, Khasanova N M, Nizamutdinov N M, Galeev A A and Rudowicz C 2000 *Appl. Magn. Reson.* at press
[24] Koster G F and Statz H 1959 *Phys. Rev.* **113** 445
[25] Buckmaster H A, Chatterjee R and Shing Y H 1972 *Phys. Status Solidi* a **13** 9
[26] Bacquet G, Dugas J, Escribe C, Gaite J M and Michoulier J 1974 *J. Phys. C: Solid State Phys.* **7** 1551
[27] Rudowicz C and Bramley R 1985 *J. Chem. Phys.* **83** 1985
[28] Rudowicz C and Madhu S B 1999 *J. Phys.: Condens. Matter* **11** 273
[29] Assa R and Vangard T 1975 *J. Magn. Reson.* **19** 308
[30] Bershov L V, Gaite J M, Hafner S S and Rager H 1983 *Phys. Chem. Miner.* **9** 95
[31] Greenwood N N and Earnshaw A 1986 *Chemistry of the Elements* (Oxford: Pergamon) p 1196
[32] Yeung Y Y and Rudowicz C 1992 *Comput. Chem.* **16** 207
[33] Chang Y M, Rudowicz C and Yeung Y Y 1994 *Comput. Phys.* **8** 583
[34] Yeung Y Y, Qin J, Chang Y M and Rudowicz C 1994 *Phys. Chem. Miner.* **21** 526
[35] Qin J, Rudowicz C, Chang Y M and Yeung Y Y 1994 *Phys. Chem. Miner.* **21** 532